



Greenhouse gases emissions from riparian wetlands: an example from the Inner Mongolia grassland region in China

Xinyu Liu^{1,2}, Xixi Lu^{1,3}, Ruihong Yu^{1,2}, Heyang Sun¹, Hao Xue¹, Zhen Qi¹, Zhengxu Cao¹, Zhuangzhuang Zhang¹, and Tingxi Liu⁴

¹Inner Mongolia Key Laboratory of River and Lake Ecology, School of Ecology and Environment, Inner Mongolia University, Hohhot 010021, China

²Key Laboratory of Mongolian Plateau Ecology and Resource Utilization, Ministry of Education, Hohhot 010021, China

³Department of Geography, National University of Singapore, 117570, Singapore

⁴Inner Mongolia Water Resource Protection and Utilization Key Laboratory, Water Conservancy and Civil Engineering College, Inner Mongolia Agricultural University, Hohhot 010021, China

Correspondence: Ruihong Yu (rhyu@imu.edu.cn) and Tingxi Liu (txliu@imau.edu.cn)

Received: 22 May 2020 – Discussion started: 28 July 2020

Revised: 22 June 2021 – Accepted: 29 July 2021 – Published: 1 September 2021

Abstract. Gradual riparian wetland drying is increasingly sensitive to global warming and contributes to climate change. Riparian wetlands play a significant role in regulating carbon and nitrogen cycles. In this study, we analyzed the emissions of carbon dioxide (CO₂), methane (CH₄), and nitrous oxide (N₂O) from riparian wetlands in the Xilin River basin to understand the role of these ecosystems in greenhouse gas (GHG) emissions. Moreover, the impact of the catchment hydrology and soil property variations on GHG emissions over time and space was evaluated. Our results demonstrate that riparian wetlands emit larger amounts of CO₂ (335–2790 mg m⁻² h⁻¹ in the wet season and 72–387 mg m⁻² h⁻¹ in the dry season) than CH₄ and N₂O to the atmosphere due to high plant and soil respiration. The results also reveal clear seasonal variations and spatial patterns along the transects in the longitudinal direction. N₂O emissions showed a spatiotemporal pattern similar to that of CO₂ emissions. Near-stream sites were the only sources of CH₄ emissions, while the other sites served as sinks for these emissions. Soil moisture content and soil temperature were the essential factors controlling GHG emissions, and abundant aboveground biomass promoted the CO₂, CH₄, and N₂O emissions. Moreover, compared to different types of grasslands, riparian wetlands were the potential hotspots of GHG emissions in the Inner Mongolian region. Degradation of downstream wetlands has reduced the soil carbon pool by approximately 60 %, decreased CO₂ emissions by approx-

imately 35 %, and converted the wetland from a CH₄ and N₂O source to a sink. Our study showed that anthropogenic activities have extensively changed the hydrological characteristics of the riparian wetlands and might accelerate carbon loss, which could further affect GHG emissions.

1 Introduction

With the increasing rate of global warming, the change in the concentrations of greenhouse gases (GHGs) in the atmosphere is a source of concern in the scientific community (Cao et al., 2005). According to the World Meteorological Organization (WMO, 2018), the concentrations of carbon dioxide (CO₂), methane (CH₄), and nitrous oxide (N₂O) in the atmosphere have increased by 146 %, 257 %, and 122 %, respectively, since 1750. Despite their lower atmospheric concentrations, CH₄ and N₂O absorb infrared radiation approximately 28 and 265 times more effectively at centennial timescales than CO₂ (IPCC, 2013), respectively. On a global scale, CO₂, CH₄, and N₂O together are responsible for 87 % of the GHG effect (Ferrón et al., 2007).

Wetlands are unique ecosystems that serve as transition zones between terrestrial and aquatic ecosystems. They play an important role in the global carbon cycle (Beger et al., 2010; Naiman and Decamps, 1997). Wetlands are sensitive to hydrological changes, particularly in the context of global

climate change (Cheng and Huang, 2016). Moreover, wetland hydrology is affected by local anthropogenic activities, such as the construction of reservoirs, resulting in gradual drying. Although wetlands cover only 4 %–6 % of the terrestrial land surface, they contain approximately 12 %–24 % of global terrestrial soil organic carbon (SOC), thus acting as carbon sinks. Moreover, they release CO₂, CH₄, and N₂O into the atmosphere and serve as carbon sources (Lv et al., 2013). During plant photosynthesis, the amount of carbon accumulated is generally higher than the amount of CO₂ consumed (plant respiration, animal respiration, and microbial decomposition) in the wetland; thus, the net effect of the wetland is that of a carbon sink. Wetlands are increasingly recognized as an essential part of nature, given their simultaneous functions as carbon sources and sinks. Excessive rainfall causes an expansion in wetland area and a sharp increase in soil moisture content, thus enhancing respiration, methanogenesis, nitrification, and denitrification rates (Mitsch et al., 2009). On the other hand, reduced precipitation or severe droughts decrease water levels, causing the wetlands to dry up. The accumulated carbon is released back into the atmosphere through oxidation. Due to the increasing impact of climate change and human activity, drying of wetlands has been widely observed in recent years (Liu et al., 2006); more than half of global wetlands have disappeared since 1900 (Mitsch and Gosselink, 2007), and this tendency is expected to continue in the future. The loss of wetlands may directly shift the soil environment from anoxic to oxic conditions, while modifying the CO₂ and CH₄ source and sink functions of wetland ecological systems (Waddington and Roulet, 2000; Zona et al., 2009).

The Xilin River basin in China is characterized by a marked spatial gradient in soil moisture content. It is a unique natural laboratory that may be used to explore the close relationships between the spatiotemporal variations in hydrology and riparian biogeochemistry. Wetlands around the Xilin River play an irreplaceable role with regard to local climate control, water conservation, the carbon and nitrogen cycles, and husbandry (Gou et al., 2015; Kou, 2018). Moreover, the Xilin River region is subjected to seasonal alterations in precipitation and temperature regimes. Construction of the Xilin River reservoir has resulted in highly negative consequences, such as the drying of downstream wetlands, thereby affecting riparian hydrology and microbial activity in riparian soils. GHG emissions in riparian wetlands vary immensely. Therefore, understanding the interactions between the GHG emissions and hydrological changes in the Xilin River riparian wetlands has become increasingly important. Moreover, it is necessary to estimate the changes in GHG emissions as a result of wetland degradation at local and global scales.

In this work, GHG emissions from riparian wetlands and adjacent hillslope grasslands of the Xilin River basin were investigated. GHG emissions, soil temperature, and soil moisture content were measured in the dry and wet seasons. The main objectives of this study were to (1) investigate the tem-

poral and spatial variations in CO₂, CH₄, and N₂O emissions from the wetlands in the riparian zone and examine the main factors affecting the GHG emissions; (2) compare the GHG emissions from the riparian wetlands with those from different types of grasslands; and (3) evaluate the impact of wetland degradation in the study area on GHG emissions.

2 Materials and methods

2.1 Study site

The Xilin River is situated in the southeastern part of the Inner Mongolia Autonomous Region in China (43°26′–44°39′ N, 115°00′–117°30′ E). It is a typical inland river of the Inner Mongolia grasslands. The river basin area is 10 542 km², total length is 268.1 km, and average altitude is 988.5 m. According to the meteorological data provided by the Xilinhot Meteorological Station (Xi et al., 2017; Tong et al., 2004), the long-term annual mean air temperature is 1.7 °C, and the maximum and minimum monthly means are 20.8 °C in July and –19.8 °C in January, respectively. The average annual precipitation was 278.9 mm for the period of 1968–2015. Precipitation is distributed unevenly among the seasons, with 87.41 % of the total precipitation occurring between May and September.

Soil types in the Xilin River basin are predominantly chernozems (86.4 %), showing a significant zonal distribution as light chestnut soil, dark chestnut soil, and chernozems from the northwest to southeast. Soil types in this basin also present a vertical distribution with elevation. Soluble chernozems and carbonate chernozems are primarily observed at altitudes above 1350 m, with a relatively fertile and deep soil layer. Dark chestnut soil, boggy soil, and dark meadow with high humus content are distributed between the altitudes of 1150 and 1350 m. Meanwhile, light chestnut soil, saline meadow soil, and meadow solonchak with low soil humus, a thin soil layer, and coarse soil texture are distributed between the altitudes of 902 and 1150 m above sea level (Xi et al., 2017).

2.2 Field measurements and laboratory analyses

In this study, five representative transects were selected as the primary measurement sites in the entire Xilin River. Each transect cuts through the riparian wetlands near the river and the hillslope grasslands further away (Fig. 1).

The layout of the sampling points of each transect is shown in Fig. 2. Each sampling point, from T1–T5, was extended from either side of the river to the grassland on the slopes by using five to seven sampling points for each transect, resulting in 24 points in total. The sampling sites on the left and right banks were defined as L1–L3 and R1–R4 from the riparian wetlands to the hillslope grasslands. As transect T3 was located on a much wider flood plain, none of its sampling points were located on the hillslope grassland. The last

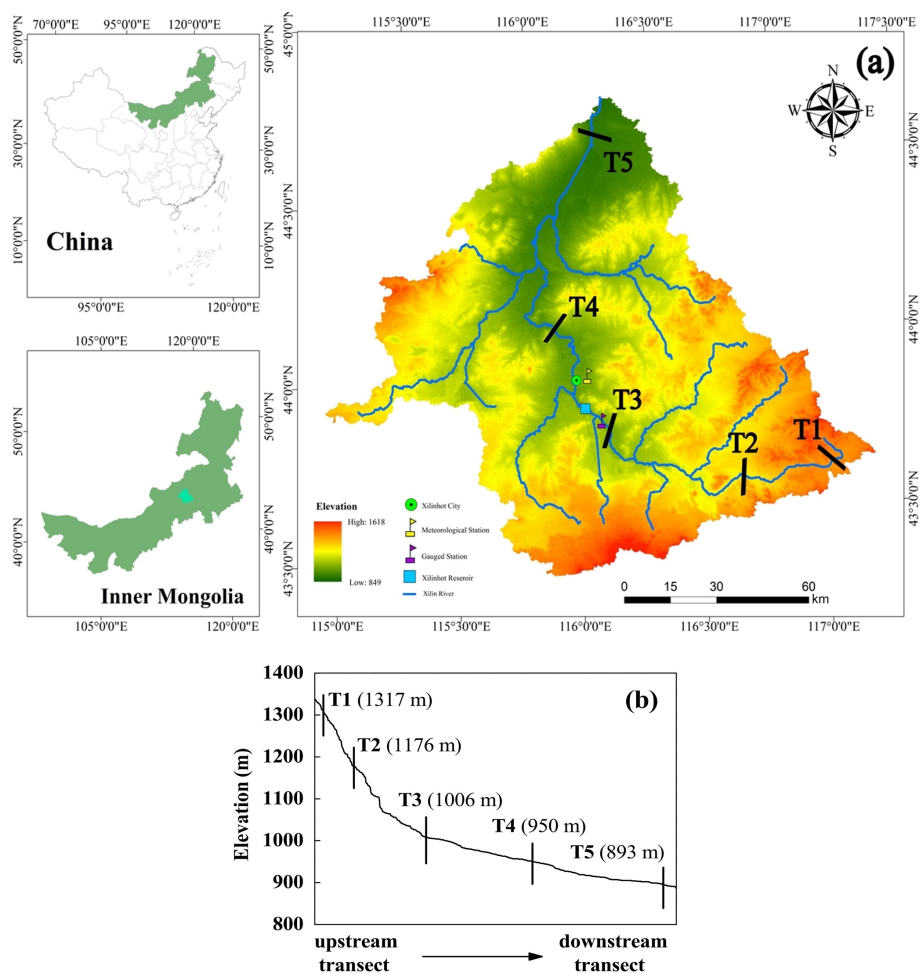


Figure 1. (a) Location of the Xilin River basin and distribution of five riparian–hillslope transects (T1–T5). (b) Elevation details of each transect in the Xilin River basin.

transect (T5) was located downstream in the dry lake and contained seven sampling points. They were defined as S1–S7, where S1, S2, and S7 were located along the lakeshore (the lakeside zone), and S3–S6 were located in the dry lake bed (S3 and S4 in the mudbank, S5 in saline–alkali soil, and S6 in sand–gravel geology). Moreover, characterizations for the T1, T2, and T3 transects were located along the continuous river flow, and the T4 and T5 transects were located along the intermittent river flow.

The CO_2 , CH_4 , and N_2O emissions from each site were measured in August (wet season) and October (dry season) in 2018 using a static dark chamber and the gas chromatography method. The static chambers were made of a cube-shaped polyvinyl chloride (PVC) pipe (dimensions: $0.4\text{ m} \times 0.2\text{ m} \times 0.2\text{ m}$). A battery-driven fan was installed horizontally inside the top wall of the chamber to ensure proper air mixing during measurements. To minimize heating from solar radiation, white adiabatic aluminum foil was used to cover the entire aboveground portion of the chamber. During measurements, the chambers were driven into the soil to

ensure airtightness and connected with a differential gas analyzer (Li-7000 $\text{CO}_2/\text{H}_2\text{O}$ analyzer, LI-COR, USA) to measure the changes in the soil CO_2 concentration. The air in the chamber was sampled using a 60 mL syringe at 0, 7, 14, 21, and 28 min. The gas samples were stored in a reservoir bag and taken to the laboratory for CH_4 and N_2O measurements using gas chromatography (GC-2030, Japan). The measurements were scheduled for 09:00–11:00 or 15:00–17:00 UTC+8.

Soil temperature (ST) was measured at depths of 0–10 and 10–20 cm with a geothermometer (DTM-461, Hengshui, China). Plant samples were collected in a static chamber and oven-dried in the laboratory to obtain aboveground biomass (BIO). A 100 cm^3 ring cutter was used to collect surface soil samples at each site, which were placed in aluminum boxes and immediately brought back to the laboratory to measure soil mass moisture content (SMC) and soil bulk density (ρ_b) using national standard methods (NATESC, 2006). Topsoil samples were collected, sealed in plastic bags, and brought back to the laboratory to measure soil pH, electrical conduc-

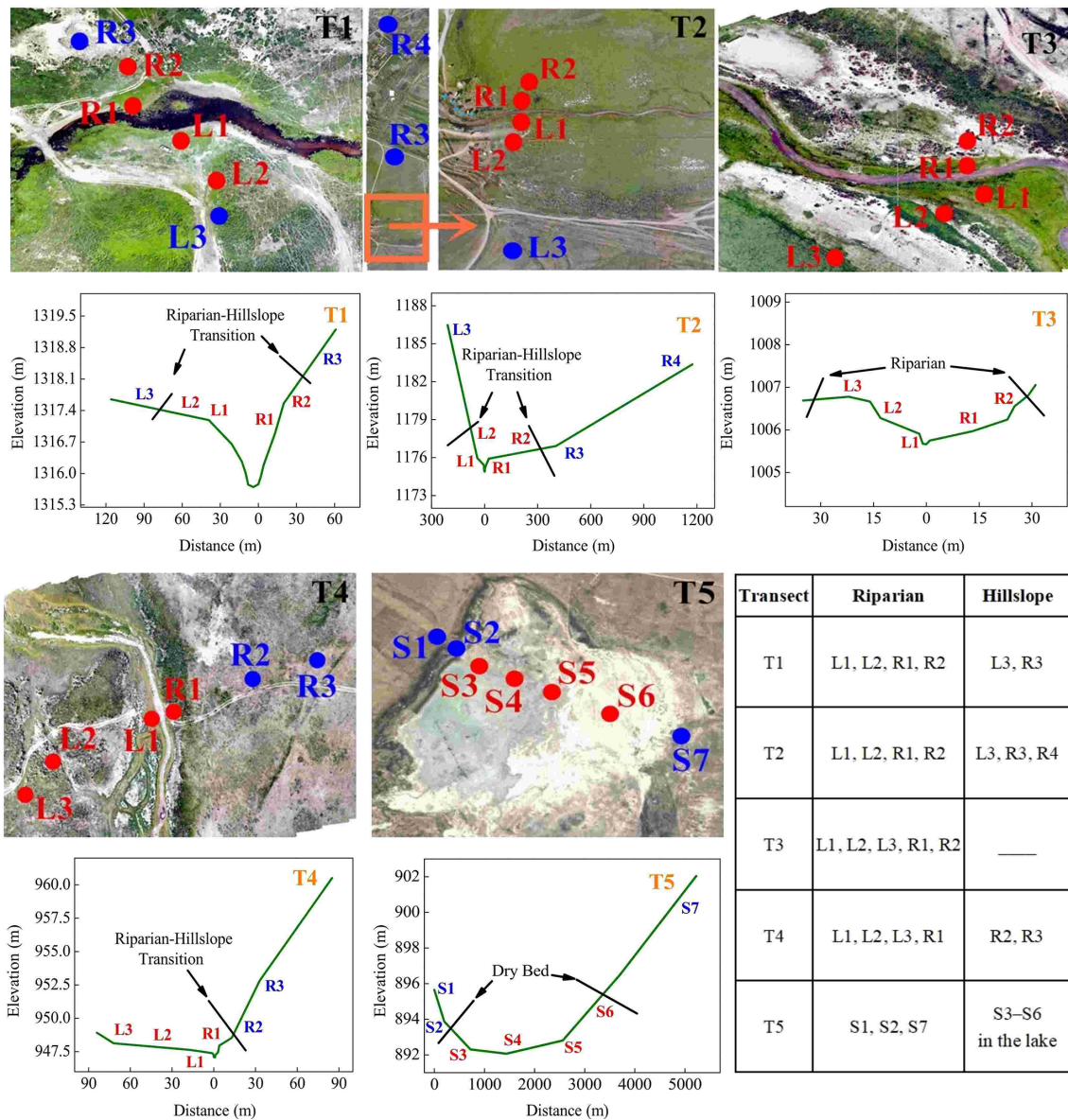


Figure 2. Distributions of sampling points in transects T1–T5 (the images are the authors’ own).

tivity (EC), total soil organic carbon (TOC) content, and soil C : N ratio.

2.3 Calculation of GHG emissions

The CO₂, CH₄, and N₂O emissions were calculated using Eq. (1) (Qin et al., 2016):

$$F = \frac{V}{A} \times \frac{dc}{dt} \times \rho = H \times \frac{dc}{dt} \times \frac{M}{V} \times \left(\frac{273.15}{273.15 + t} \right), \quad (1)$$

where *F* denotes the flux of CO₂, CH₄, and N₂O emissions (mg m⁻² h⁻¹); *H* is the height of the static chamber (0.18 m); *M* is the relative molecular weight (44 for CO₂ and N₂O, and 16 for CH₄); *V* is the volume of gas in the standard state

(22.4 L mol⁻¹); *dc/dt* is the rate of change of the gas concentration (10⁻⁶ h⁻¹); and *T* is the temperature in the black chamber (°C).

The annual cumulative emissions were calculated using Eq. (2) (Whiting and Chanton, 2001):

$$M = \sum \frac{F_{i+1} + F_i}{2} \times (t_{i+1} - t_i) \times 24, \quad (2)$$

where *M* denotes the total cumulative emission amounts of CO₂, CH₄, or N₂O (kg hm²); *F* is the emission flux of CO₂, CH₄, or N₂O; *i* is the sampling frequency; and *t_{i+1} - t_i* represents the interval between two adjacent measurement dates.

In this study, a 100-year timescale was selected to calculate the global warming potential (GWP) of soil CH₄ and

Table 1. Physical and chemical properties (mean \pm SD) of soils at various sites within each transect.

Transect	Zone	Sample number	SMC10-V	SMC20-V	Soil C : N	TOC (g kg ⁻¹)	BIO (g)	ρ_b	pH	EC ($\mu\text{S cm}^{-1}$)	SSM (%)
T1	Riparian	12	12.16 \pm 7.55	12.88 \pm 12.05	12.46 \pm 0.91	30.16 \pm 6.54	14.67 \pm 5.44	1.28 \pm 0.07	7.25 \pm 0.62	154.71 \pm 23.70	47.77 \pm 7.04
	Hillslope	6	2.72 \pm 0.91	5.05 \pm 3.09	11.41 \pm 0.09	10.77 \pm 4.72	6.70 \pm 1.48	1.45 \pm 0.03	7.22 \pm 0.40	82.02 \pm 16.37	31.02 \pm 1.32
T2	Riparian	12	26.75 \pm 19.52	12.19 \pm 7.82	11.70 \pm 1.14	19.96 \pm 5.71	24.76 \pm 9.65	1.23 \pm 0.05	8.95 \pm 0.45	303.88 \pm 102.16	51.21 \pm 6.49
	Hillslope	9	5.85 \pm 4.82	3.03 \pm 1.43	9.77 \pm 0.88	14.87 \pm 11.21	6.10 \pm 3.19	1.38 \pm 0.13	8.10 \pm 0.55	162.97 \pm 128.18	35.09 \pm 6.75
T3	Riparian	12	28.04 \pm 22.95	14.53 \pm 8.98	15.80 \pm 4.16	22.40 \pm 9.69	6.37 \pm 2.95	1.35 \pm 0.19	9.50 \pm 0.67	1233.20 \pm 829.83	47.56 \pm 11.65
	L3	3	116.37 \pm 56.91	113.36 \pm 23.17	16.8 \pm 0.58	36.1 \pm 1.84	107.75 \pm 16.94	0.592 \pm 0.02	8.5 \pm 0.17	403 \pm 57.21	> 100
T4	Riparian	12	5.42 \pm 3.34	4.07 \pm 4.31	12.52 \pm 2.06	9.96 \pm 1.25	11.97 \pm 4.50	1.30 \pm 0.08	8.84 \pm 0.22	461.72 \pm 314.27	44.08 \pm 7.07
	Hillslope	6	3.35 \pm 2.06	4.27 \pm 1.94	9.97 \pm 0.50	9.65 \pm 1.05	7.84 \pm 2.48	1.30 \pm 0.09	8.23 \pm 0.14	118.5 \pm 8.25	39.43 \pm 5.55
T5	Dry lake bed	12	17.47 \pm 15.08	14.49 \pm 13.28	63.74 \pm 12.93	31.41 \pm 6.55	5.48 \pm 2.35	1.16 \pm 0.10	9.88 \pm 0.18	7320.87 \pm 4300.03	58.47 \pm 7.16
	Lakeshore	9	2.64 \pm 1.48	2.82 \pm 1.27	15.92 \pm 4.71	6.35 \pm 1.16	0	1.33 \pm 0.09	9.41 \pm 0.7	281.82 \pm 162.73	37.52 \pm 5.34

Note: SMC10-V – soil volumetric moisture content in 0–10 cm; SMC20-V – soil volumetric moisture content in 10–20 cm; soil C : N – soil carbon–nitrogen ratio; TOC – total soil organic carbon; BIO – aboveground biomass; ρ_b – soil bulk density; pH – soil pH; EC – soil electrical conductivity; SSM – saturated soil moisture.

N₂O emissions (Whiting and Chanton, 2001):

$$\text{GWP} = 1 \times [\text{CO}_2] + 25 \times [\text{CH}_4] + 298 \times [\text{N}_2\text{O}], \quad (3)$$

where 25 and 298 are the GWP multiples of CH₄ and N₂O relative to CO₂ on a 100-year timescale, respectively.

2.4 Statistical analysis

All statistical analyses were performed using SPSS for Windows version 18.0 (SPSS Inc., Chicago, IL, USA). Statistical significance was set at $P < 0.05$. Pearson correlation analysis was conducted to estimate the relationships between GHG fluxes and environmental variables. A Wilcoxon test was used to determine the differences in the GHG fluxes between the two seasons.

3 Results

3.1 Spatiotemporal patterns of SMC for each transect

The temporal and spatial variations in SMC10 occurred in the following order: wet season > dry season and riparian wetlands > hillslope grasslands (Fig. 3a, c, and e). Similar variations were observed in SMC20 (Fig. 3b, d, and f). The average SMC10 and SMC20 in the continuous river transects in the riparian zones (SMC10 values were 37.44 % in the wet season and 19.40 % in the dry season, while SMC20 values were 25.96 % in the wet season and 17.39 % in the dry season) were higher than those in the hillslope grasslands (SMC10 values were 9.12 % in the wet season and 4.15 % in the dry season; SMC20 values were 6.51 % in the wet season and 5.96 % in the dry season). During the study period, both SMC10 and SMC20 changed as the distance from the river increased, and the highest value was observed at the near-stream sites (L1 and R1). SMC10 fluctuations were low in the intermittent transect compared with those in the upstream transects, with mean values being 11.79 % in the wet season and 3.72 % in the dry season in the riparian areas. The mean SMC10 in the hillslopes was 6.58 % in the wet season and 2.86 % in the dry season. SMC20 showed similar fluctuation; it was 7.22 % in the wet season and 2.98 % in the dry season in the riparian areas and 7.56 % in the wet season and 4.4 % in the dry season in the hillslopes. In transect T5, average SMC10 and SMC20 at the center of the lake (SMC10 values were 29.00 % in the wet season and 13.36 % in the dry season; SMC20 values were 29.30 % in the wet season and 9.69 % in the dry season) were higher than those along the lakeshore (SMC10 values were 4.90 % in the wet season and 3.13 % in the dry season; SMC20 values were 3.34 % in the wet season and 5.22 % in the dry season).

3.2 Spatiotemporal patterns of ST in each transect

Spatiotemporal differences in ST during the entire observation period are displayed in Fig. 4. ST variations in the wet

Table 2. Soil particle composition of soils at various sites within each transect.

Transect	Zone	Soil particle composition		
		Clay % (< 0.002 mm)	Silt % (0.02 – 0.002 mm)	Sand (2.0 – 0.02 mm)
T1	Riparian	2.5	2.7	94.8
	Hillslope	9.6	6.1	85.3
T2	Riparian	5.5	5.8	90.7
	Hillslope	10.8	8.6	80.6
T3	Riparian	4.1	1.1	94.8
T4	Riparian	11.4	1.5	87.1
	Hillslope	12.7	5.9	81.4
T5	Lakeshore	5.1	2.1	92.8
	Dry lake bed	46.1	4.8	49.1

season (mean was 27.4 °C) were noticeably higher than those in the dry season (mean was 8.97 °C). Moreover, ST at riparian sites (mean, 26.0 °C in the wet season and 8.41 °C in the dry season) was slightly lower than that at the hillslope grasslands (mean, 30.9 °C in the wet season and 10.3 °C in the dry season) for the 0–10 cm soil depth, with the exception of transect T5. Similar results were observed for the 10–20 cm soil depth.

3.3 Spatiotemporal patterns of GHG emissions in each transect

Figure 5 shows the spatiotemporal variations in GHG emissions in the wet and dry seasons in each transect. CO_2 emissions in each transect were higher in the wet season than in the dry season. The average emissions in the riparian wetland transects T1–T4 (1582.09 ± 679.34 $\text{mg m}^{-2} \text{h}^{-1}$ in the wet season and 163.24 ± 84.98 $\text{mg m}^{-2} \text{h}^{-1}$ in the dry season) were higher than the transects in the hillslope grasslands (1071.54 ± 225.39 $\text{mg m}^{-2} \text{h}^{-1}$ in the wet season and 77.68 ± 25.32 $\text{mg m}^{-2} \text{h}^{-1}$ in the dry season). High CO_2 fluxes occurred in the riparian zones, while lower CO_2 fluxes were observed in the hillslope grasslands in continuous river transects (T1, T2, and T3). Transect T4 exhibited lower CO_2 emission in the riparian wetlands near the channel than at sites away from the channel. CO_2 emissions in transect T5 in the wet and dry seasons decreased from the lakeshore to the lake center.

CH_4 emissions at the continuous river flow transects (T1, T2, and T3) varied between the wet and dry seasons, except for those at T4 (characterized by intermittent river flow) and T5 (the dry lake). In the wet season, the near-stream sites (L1 and R1) in T1, T2, and T3 were characterized as high- CH_4 sources (average, 3.74 ± 3.81 $\text{mg m}^{-2} \text{h}^{-1}$), but the sites located away from the river gradually turned into CH_4 sinks. Moreover, all the sites in transects T4 and T5 were sinks. CH_4 emissions (mean value: 0.2 ± 0.45 $\text{mg m}^{-2} \text{h}^{-1}$)

at the wetland sites were always lower in the dry season than those in the wet season. However, the sites on the hillslope grasslands served as CH_4 sinks (mean value: -0.05 ± 0.03 $\text{mg m}^{-2} \text{h}^{-1}$). In transect T5, CH_4 emissions showed the opposite trend; a CH_4 sink was observed in the wet season, but it was transformed into a CH_4 source in the dry season.

Similar to the CO_2 and CH_4 emissions, N_2O emissions showed a distinct spatiotemporal pattern in all the transects. N_2O emissions in the wet season were higher than those in the dry season. These emissions were higher in the riparian wetlands than in the hillslope grasslands. Moreover, almost all sites with continuous river flow were N_2O sources, while more than half of the sites with intermittent river flow were sinks.

Table 3 shows that CO_2 fluxes were significantly correlated between the wet and dry seasons, while CH_4 and N_2O fluxes were not correlated between the two seasons.

3.4 Spatiotemporal patterns of GHG emission in upstream and downstream areas

Figure 6 shows the detailed spatial and seasonal patterns of GHG emission in the wet and dry seasons in the longitudinal direction from the upstream (T1, T2, and T3) to the downstream areas (T4 and T5). The CO_2 , CH_4 , and N_2O emissions were calculated using the average values of the respective emissions in the wetlands and hillslope grasslands in each transect.

CO_2 emissions at the riparian wetlands (Fig. 6a) in the wet season decreased from 2444.69 ± 228.58 $\text{mg m}^{-2} \text{h}^{-1}$ in the upstream area to 665.08 ± 347.57 $\text{mg m}^{-2} \text{h}^{-1}$ downstream, and the corresponding values for the dry season were 238.12 ± 48.20 and 94.14 ± 7.67 $\text{mg m}^{-2} \text{h}^{-1}$, respectively. However, in the hillslope grasslands (Fig. 6b), CO_2 emissions exhibited no significant seasonality between the upstream and downstream areas, with mean values being 1103.40 ± 190.44 $\text{mg m}^{-2} \text{h}^{-1}$ in the wet season and

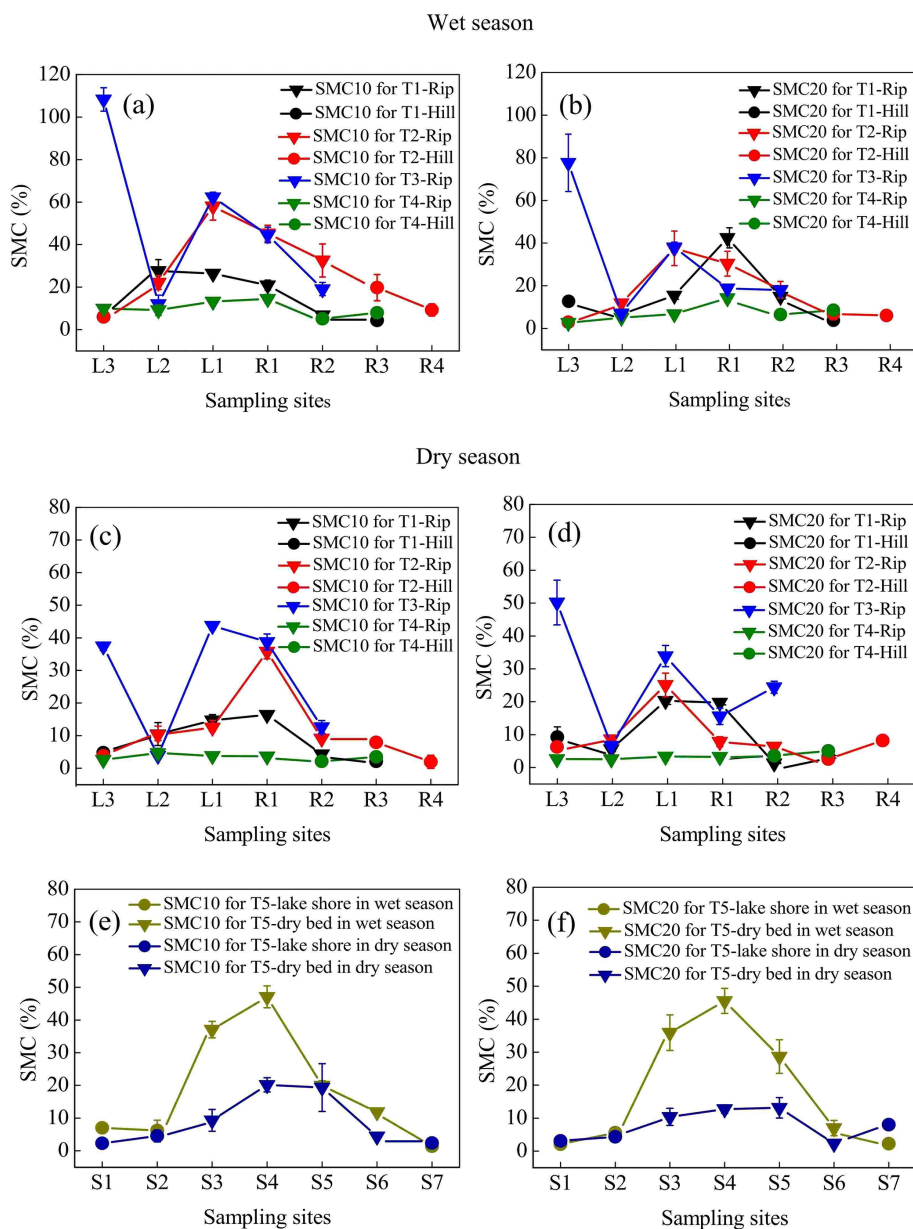


Figure 3. Soil mass moisture contents (SMCs) at soil depths of 0–10 cm (SMC10) and 10–20 cm (SMC20) for transects T1–T5 in the wet and dry seasons. Error bars represent the SD about the mean.

$79.18 \pm 24.52 \text{ mg m}^{-2} \text{ h}^{-1}$ in the dry season. In addition, the CO_2 emissions in transect T5 were low for both months, with averages of $162.83 \pm 149.15 \text{ mg m}^{-2} \text{ h}^{-1}$ and $63.26 \pm 12.40 \text{ mg m}^{-2} \text{ h}^{-1}$ in the wet and dry seasons, respectively. The upstream riparian zones exhibited higher CO_2 emissions ($894.32 \pm 868.47 \text{ mg m}^{-2} \text{ h}^{-1}$) than their downstream counterparts ($621.14 \pm 704.10 \text{ mg m}^{-2} \text{ h}^{-1}$). Mean CO_2 emissions showed no significant differences in the grasslands, averaging $524.16 \pm 450.10 \text{ mg m}^{-2} \text{ h}^{-1}$ upstream and $508.06 \pm 534.77 \text{ mg m}^{-2} \text{ h}^{-1}$ downstream.

CH_4 emissions showed a marked spatial pattern in the riparian zones from upstream to downstream (Fig. 6c).

The transects with continuous river flow were CH_4 sources in the wet and dry seasons, with average emissions of 1.42 ± 3.41 and $0.27 \pm 0.49 \text{ mg m}^{-2} \text{ h}^{-1}$, respectively; while those with intermittent river flow served as CH_4 sinks, with the corresponding means of -0.21 ± 0.45 and $-0.02 \pm 0.05 \text{ mg m}^{-2} \text{ h}^{-1}$, respectively. Moreover, the hillslope grassland sites in all transects were CH_4 sinks (Fig. 6d).

N_2O emissions in riparian wetlands (Fig. 7e) showed spatial patterns similar to those of CH_4 emissions. In the wet season, the transects with continuous river flow served as N_2O sources, with a mean emission of $0.031 \pm 0.031 \text{ mg m}^{-2} \text{ h}^{-1}$; meanwhile, transects with intermittent

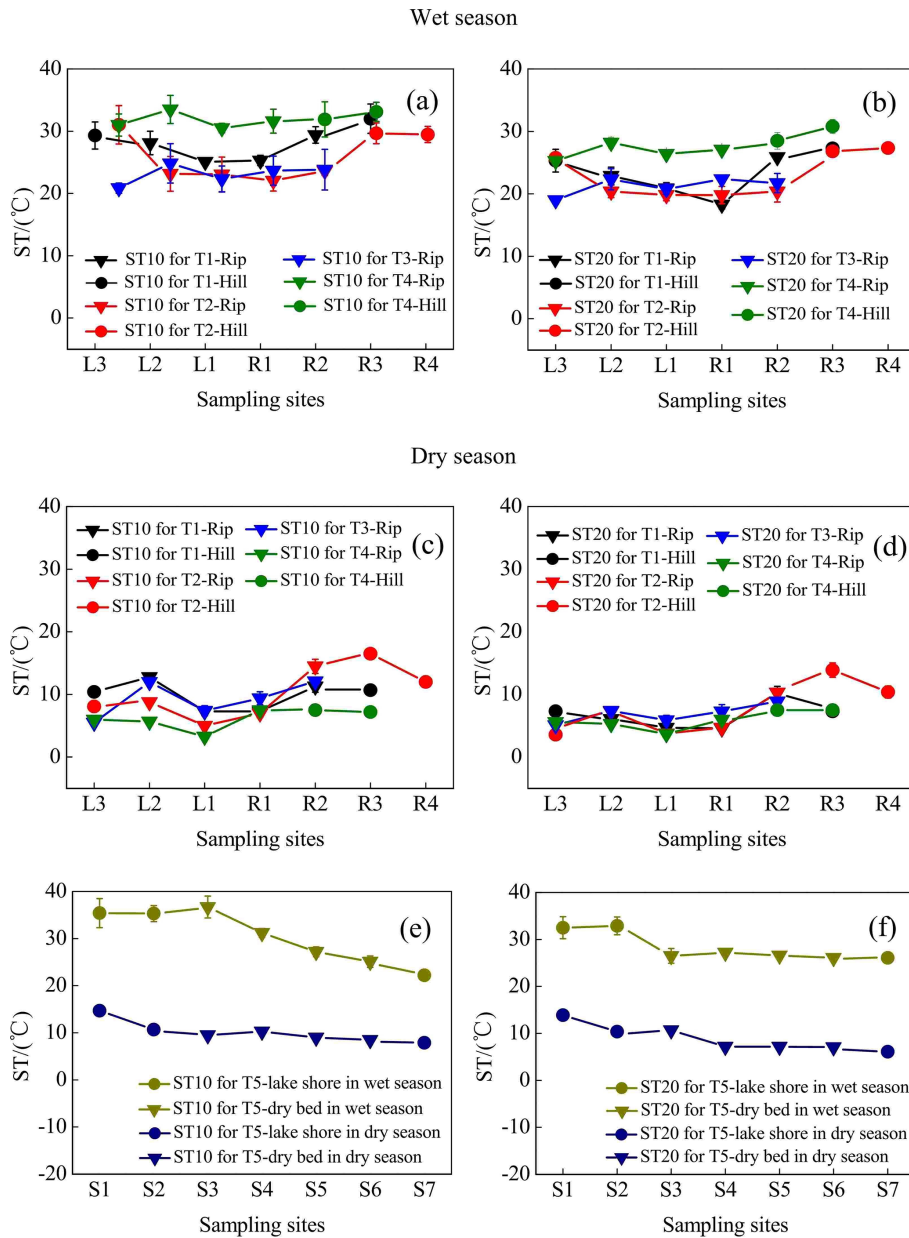


Figure 4. Soil temperatures (STs) at soil depths of 0–10 cm (ST10) and 10–20 cm (ST20) for transects T1–T5 in the wet and dry seasons. Error bars represent the SD about the mean.

Table 3. Significant correlations between GHGs fluxes and two seasons ($n = 31$).

GHG flux	FCO_2 in the wet season – FCO_2 in the dry season	FCH_4 in the wet season – FCH_4 in the dry season	FN_2O in the wet season – FN_2O in the dry season
Significant correlations (P)	0.000	0.133	0.290

Note: $P < 0.05$ denotes significant correlation and $P > 0.05$ denotes no significant correlation.

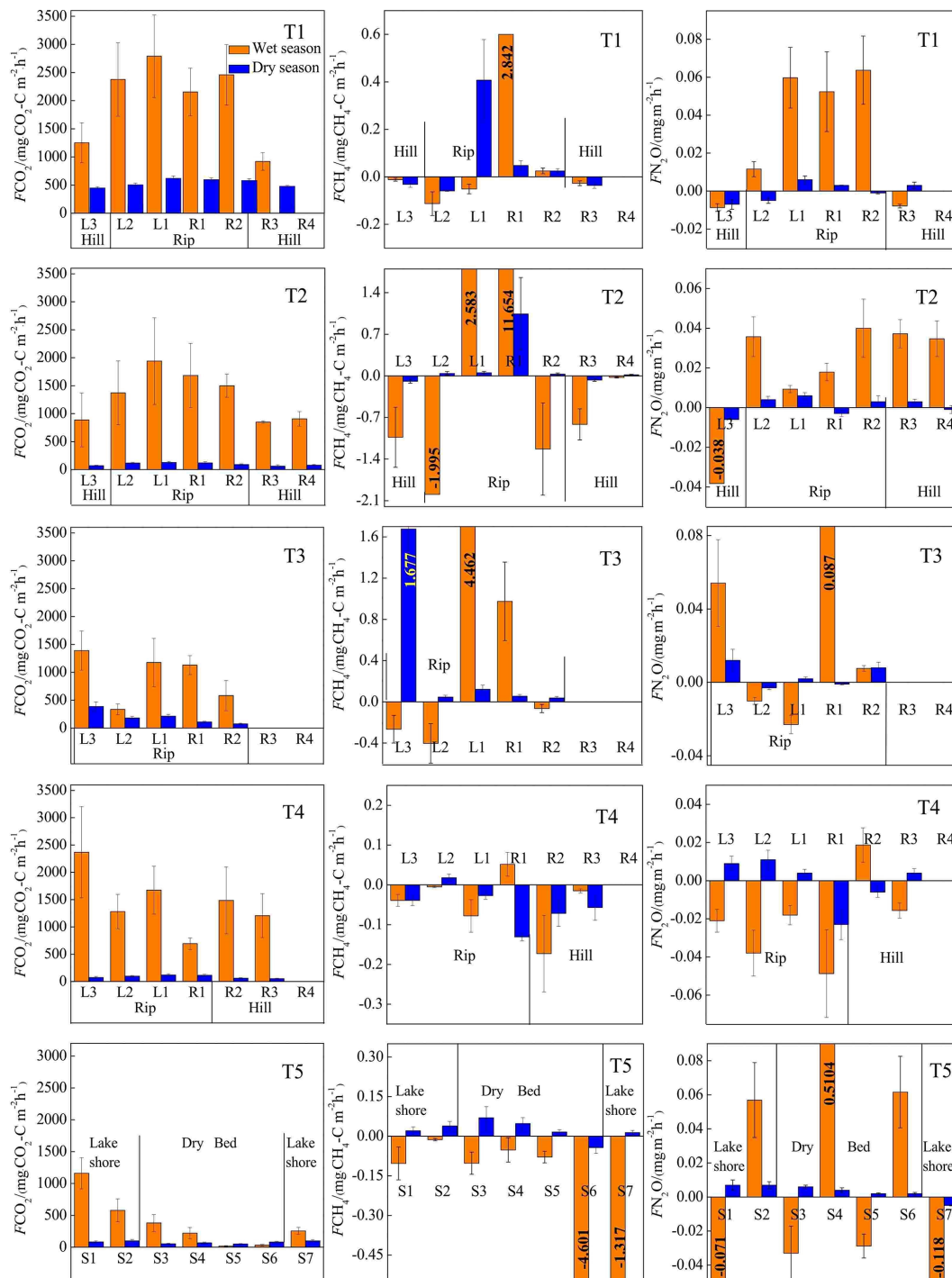


Figure 5. Spatiotemporal patterns of CO₂ (first column), CH₄ (second column), and N₂O (third column) emission (*F*) for each transect. Data are shown for the wet season (orange) and the dry season (blue). Error bars depict standard deviation.

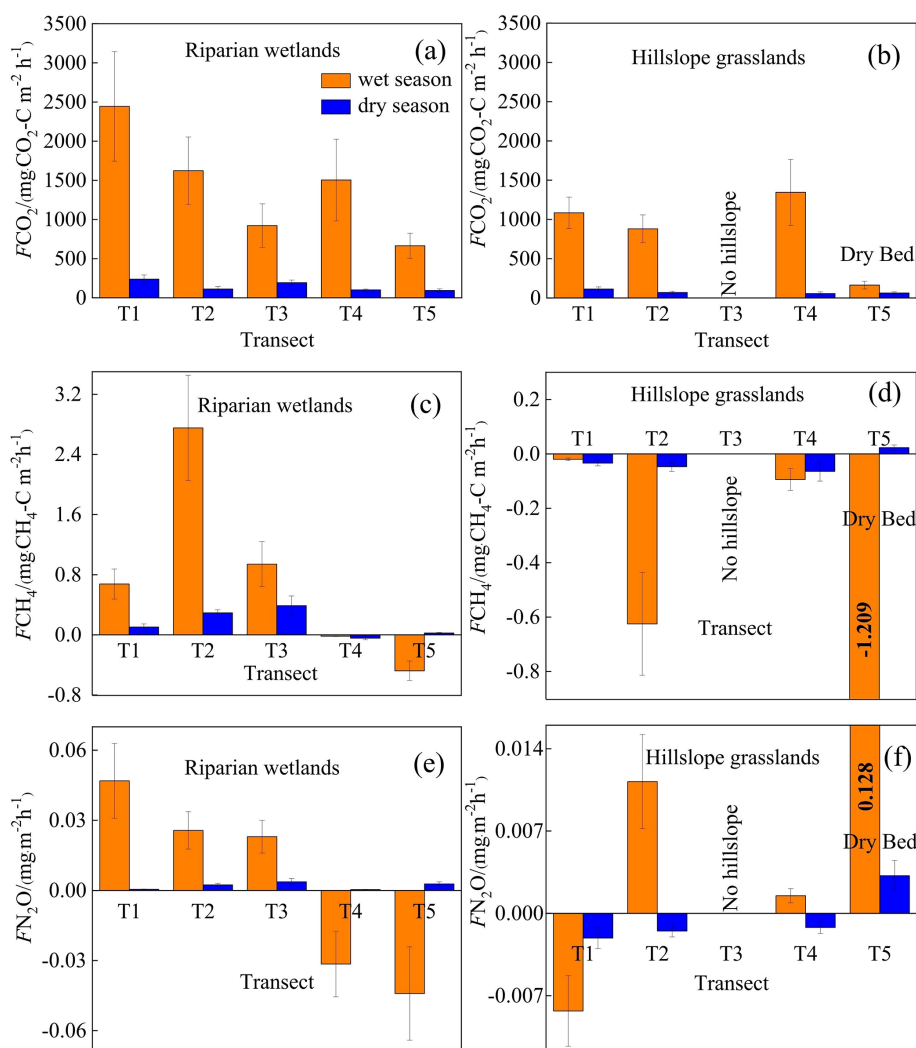


Figure 6. Spatiotemporal patterns of CO₂ (first line), CH₄ (second line), and N₂O (third line) emissions (F) in the upstream (T1, T2, and T3) and downstream areas (T4 and T5). Bars represent the mean values for each transect, and error bars show the standard errors.

river flow acted as N₂O sinks with an average emission of $-0.037 \pm 0.05 \text{ mg m}^{-2} \text{ h}^{-1}$. In the dry season, N₂O emissions occurred as weak sources in the longitudinal transects, exhibiting an average emission of $0.002 \pm 0.007 \text{ mg m}^{-2} \text{ h}^{-1}$. However, the N₂O emission in the hillslope grasslands did not show any spatial patterns (Fig. 7f).

4 Discussion

4.1 Main factors influencing GHG emissions

4.1.1 Effects of SMC on GHG emissions

SMC constitutes one of the main factors affecting GHG emission in wetlands. In this study, transects T1–T4 were characterized by a marked spatial SMC gradient (i.e., a gradual decrease in SMC10 and SMC20 from the riparian wet-

lands to the hillslope grasslands and from the upstream to downstream regions; Fig. 3). The CO₂, CH₄, and N₂O emissions showed a similar trend. Table 4 shows that SMC10 is positively correlated with CO₂ emission ($P < 0.05$) and that SMC10 and SMC20 are significantly positively correlated with CH₄ emission ($P < 0.01$) and with N₂O emission ($P < 0.05$ and $P < 0.01$, respectively). These results indicate the influence of wetland SMC on GHG emission.

Typically, the optimal SMC associated with CO₂ emission in the riparian wetlands ranges from 40 % to 60 % (Sjögersten et al., 2006), creating better soil aeration, and improving soil microorganism activity and respiration in plant roots, thereby promoting CO₂ emission. Excessive SMC reduces soil gas transfer due to the formation of an anaerobic environment in the soil, and microbial activity is lowered, favoring the accumulation of organic matter (Hui, 2014). The SMC of the hillslope grasslands was found to be less than 10 %. Low

to increased respiration and consequently higher CO₂ emission (Heilman et al., 1999). Previous studies have reported that ST partially controls seasonal CO₂ emission patterns (Inubushi et al., 2003). Concurrently, CO₂ emissions in the wet season were significantly higher than those in the dry season in this study.

CH₄ emissions showed a clear seasonal pattern, likely because high summer temperatures improve the activity of both CH₄-producing and CH₄-oxidizing bacteria (Ding et al., 2010). However, as Table 4 indicates, the correlation between CH₄ emission and temperature was not significant in this study, likely because SMC was a more critical factor than temperature in our study region given its very dry climate. SMC showed a positive correlation with GHG emissions. In addition, SMC affected ST to a certain extent, while the interactions between SMC and ST had a mutual influence on CH₄ emission. During the study period, the near-stream sites (L1 and R1) maintained a super-wet state on the ground surface for a long time, which was beneficial for the production of CH₄. However, the wetlands maintained a state without water accumulation on the soil surface in August, which was conducive to the oxidative absorption of CH₄. SMC thus masked the effect of ST on CH₄ emissions.

Previous studies have indicated that temperature is an important factor affecting N₂O emission (Sun et al., 2011) through primary mechanisms impacting the nitrifying and denitrifying bacteria in the soil. As Table 4 shows, the correlations between N₂O emission and ST10 and ST20 were poor ($P > 0.05$). This can be attributed to the wide suitable temperature range for nitrification–denitrification and weak sensitivity to temperature. Malhi and McGill (1982) found that the optimum temperature for nitrification was 20 °C and that it inhibits entirely at 30 °C. However, Brady (1999) believed that the suitable temperature range for nitrification is 25–35 °C and that nitrification inhibits below 5 °C or above 50 °C. This shows that the temperature requirements of nitrifying microorganisms in wetland soils are possibly different in different temperature belts. The suitable temperature range was the performance of the long-term adaptability of nitrifying microorganisms. Meanwhile, several studies have revealed that denitrification can be carried out in a wide temperature range (5–70 °C) and that it is positively related to temperature (Fan, 1995). However, the process is inhibited when the temperature is too high or too low. The average ST in the wet season was 27.4 °C, conducive to the growth of denitrifying microorganisms, while that in the dry season was 8.97 °C, and the microbial activity was generally low (Sun et al., 2011). Furthermore, ST fluctuations were low in both the wet and dry seasons. Therefore, the effect of ST on N₂O emission may have been masked by other factors, such as moisture content.

4.1.3 Effects of BIO and soil organic matter content on GHG emissions

CO₂ and CH₄ emissions were higher in the riparian wetlands than in the grasslands, mainly because of the greater vegetation cover in the former. Typically, CO₂ emissions in the riparian wetlands originate from plants and microorganisms, with plant respiration accounting for a large proportion in the growing season. Previous studies have shown that plant respiration accounts for 35 %–90 % of the total respiration in the wetland ecosystem (Johnson-Randall and Foote, 2005). The good soil physicochemical properties and high soil TOC content of the riparian wetlands improve both the activity of soil microorganisms and plant root respiration. As Table 4 shows, BIO is significantly correlated with CO₂ ($P < 0.05$) and CH₄ ($P < 0.01$) emissions. These results are indicated by the significant linear positive correlation between the respiration rate and plant biomass (Lu et al., 2007). Higher plant biomass storage can achieve more carbon accumulation during photosynthesis and higher exudate release by the roots. This, in turn, promotes the accumulation of soil organic matter. An increased amount of organic matter stimulates the growth and reproduction of soil microorganisms, ultimately promoting CO₂ and CH₄ emission. Moreover, plants act as gas channels for CH₄ transmission, and a larger amount of biomass promotes CH₄ emission, given the increased number of channels. In transect T3, the high CO₂ emission observed at site L3 can be attributed to the relatively high levels of SMC, BIO, and soil nutrients, which stimulate microbial respiration rates.

BIO had a weak correlation with N₂O emission (Table 4), which indicates that plants increase N₂O production and emission, although this may not be the most critical factor. Previous studies have reported mechanisms wherein the plants are able to absorb the N₂O produced in the soil through the root system before releasing it into the atmosphere. Additionally, the root exudates of plants can enhance the activity of nitrifying and denitrifying bacteria in the soil, ultimately promoting the production of N₂O. Finally, oxygen stress caused by plant respiration can regulate the production and consumption of N₂O in the soil, eventually affecting the conversion of nitrogen in the soil (Koops et al., 1996; Azam et al., 2005).

Site L3 in transect T3 was covered by tall reeds, and its BIO was much higher than that of any of the other sites; thus, the data for this site were excluded from the correlation analysis.

Soil C : N ratio refers to the ratio of the concentration of biodegradable carbonaceous organic matter to nitrogenous matter in the soil, and it forms a soil matrix with TOC. TOC decomposition provides energy for microbial activity, while the C : N ratio affects the decomposition of organic matter by soil microorganisms (Gholz et al., 2000). The correlation results (Fig. 8) indicate that TOC had a weak positive correlation with CO₂ emission ($P > 0.05$), but the soil C : N

ratio had a significant negative correlation with CO₂ emission ($P < 0.05$), indicating that nitrogen has a limiting effect on soil respiration by affecting microbial metabolism. Liu (2019) have reported that N addition promotes CO₂ emission from wetlands soil, and the effect of organic N input was significantly higher than that of inorganic N input. Organic carbon acts as a carbon source for the growth of plants and microorganisms, which boosts their respiration. Moreover, TOC has a significant correlation with N₂O emissions ($P < 0.05$). Most heterotrophic microorganisms use soil organic matter as carbon and electron donors (Morley and Baggs, 2010). Soil carbon sources have an important influence on microbial activity. Nitrifying or denitrifying microorganisms need organic matter to act as the carbon source during the assimilation of NH₃ or NO₃⁻. High content of organic matter in the soil can promote the concentration of heterotrophic nitrifying bacteria, consume dissolved oxygen in the medium, and cause the soil to become more anaerobic, thereby slowing down autotrophic growth nitrifying bacteria. This reduces the nitrification rate, ultimately promoting N₂O release. Enwall et al. (2005) studied the effect of long-term fertilization on soil denitrification microbial action intensity. They found that the soil with long-term organic fertilizer application has a significant increase in organic matter content and consequently a significant increase in denitrification activity. Typically, low soil C : N ratios are favorable for the decomposition of microorganisms, the most suitable range being between 10 and 12 (Pierzynski et al., 2005). As Table 4 shows, N₂O emission was significantly related to the soil C : N ratios ($P < 0.05$), which means that denitrifying bacteria could use their endogenous carbon source for denitrification when the external carbon source was insufficient. Moreover, incomplete denitrification leads to the accumulation of NO₂-N, which is conducive to N₂O release. Meanwhile, due to the weak competitive ability of Nos to electrons, a low soil C : N ratio inhibits the synthesis of Nos, which is also a reason for N₂O release. In this study, all sites in transects T1–T4 exhibited similar soil C : N ratios in the optimum range (Table 1), which is favorable for microbial decomposition. However, the soil C : N ratios in transect T5 were higher than those in the other transects, especially in the dry lake bed. Therefore, transect T5 showed severe mineralization and a low microbial decomposition rate.

4.2 Riparian wetlands as hotspots of GHG emissions

The results of this study emphasized that the rate of CO₂ emission in the riparian wetlands was higher than that in the hillslope grasslands, owing to a variety of factors. ST is an important factor affecting GHG emission. McInain and Martens (2006) showed that seasonal fluctuations in ST and SMC in semi-arid regions have important effects on CO₂, CH₄, and N₂O emissions in riparian soils. Poblador et al. (2017) studied the GHG emission in forest riparian zones and suggested that the difference in the CO₂ and N₂O emis-

sions in these zones is caused by the spatial gradient of the regional SMC. In this study, the upstream riparian wetlands were characterized by higher TOC content, lower soil C : N ratio, and more abundant BIO than those in the hillslope grasslands (Table 1). These soil conditions benefited the soil microbial activity, ultimately enhancing respiration as well as CO₂ emissions. However, the CO₂ emission in the downstream areas was nearly identical to that in the grasslands, likely because the wetlands gradually evolved into grasslands after their degradation. N₂O emission showed spatial patterns similar to that of CO₂ emission, likely because the CO₂ concentration was closely related to the nitrification and denitrification processes. High CO₂ concentrations can promote the carbon and nitrogen cycles in soil (Azam et al., 2005), increasing belowground C allocation, which is associated with increased root biomass, root turnover, and root exudation. Elevated *p*CO₂ in plants provides the energy for denitrification in the presence of high available N, and there is increased O₂ consumption under elevated *p*CO₂ (Baggs et al., 2003). Moreover, soil respiration increases during soil denitrification (Liu et al., 2010; Christensen et al., 1990). In this study, a weak correlation was observed between the CO₂ and CH₄ emissions in the riparian zones ($r = 0.228$), but CO₂ emission was significantly correlated with N₂O emission ($r = 0.322$, $P < 0.05$). The soil became anaerobic in the riparian areas as the SMC increased, and this was conducive to the survival of CH₄-producing bacteria and to denitrification reactions, eventually leading to an increase in CH₄ and N₂O emissions. Jacinthe et al. (2015) reported that inundated grassland-dominated riparian wetlands were CH₄ sinks (-1.08 ± 0.22 kg CH₄-C ha⁻¹ yr⁻¹), and Lu et al. (2015) also indicated that grasslands were CH₄ sinks. In our study, a marked water gradient across the transects led to the transformation of the soil from anaerobic to aerobic soil, which changed the wetland to either a CH₄ source or sink. Therefore, during the transition from the riparian wetlands to the hillslope grasslands, CH₄ sources only appeared in the near-stream sites, while sinks appeared at other sites.

Further, we compared the GHG emissions in the riparian wetlands and the hillslope grasslands around the Xilin River basin with those in various types of grasslands (meadow grassland, typical grassland, and desert grassland) in the Xilingol League in Inner Mongolia (Table 5). CO₂ emission in the wet season decreased in the following order: upstream riparian wetlands > downstream riparian wetlands > hillslope grasslands > meadow grassland > typical grassland > desert grassland. Moreover, the upper riparian wetlands acted as sources of CH₄ emission, while the downstream transects and grasslands served as CH₄ sinks. Similarly, except in the downstream transects, N₂O emissions occurred as weak sources in different types of grasslands and upstream riparian wetlands. The GHG emissions showed similar spatial patterns in October. Although these estimates were made only in the growing season in August and the non-growing season in October, our results suggest that the riparian wet-

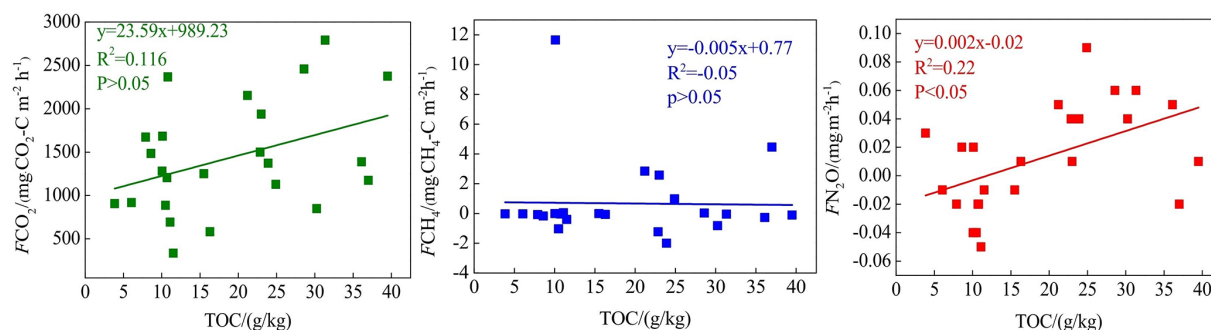


Figure 8. Correlations between soil organic carbon (TOC) content and GHG emission (F).

Table 4. Correlations between CO_2 , CH_4 , and N_2O emissions and impact factors ($n = 62$).

GHG flux	ST10	ST20	SMC10	SMC20	TOC	ρ_b	C : N	pH	EC	BIO
CO_2	0.634 ^b	0.592 ^b	0.307 ^a	0.216	0.393	-0.463 ^b	-0.289 ^b	-0.350 ^b	-0.251 ^a	0.491 ^a
CH_4	-0.029	-0.051	0.346 ^b	0.353 ^b	-0.02	-0.129	-0.156	-0.127	-0.107	0.607 ^b
N_2O	0.127	0.118	0.304 ^a	0.356 ^b	0.493 ^a	-0.194	0.311 ^a	0.137	0.504 ^b	0.251

Note: 1. The analysis method used in the table is Pearson correlation analysis, and the numbers represent Pearson correlation coefficients. 2. ^a and ^b denote significant and highly significant correlations ($P < 0.05$ and $P < 0.01$), respectively. 3. ST – soil temperature, SMC – soil moisture content, ρ_b – soil bulk density, soil C : N – soil carbon–nitrogen ratio, pH – soil pH, EC – soil electrical conductivity, and BIO – aboveground biomass.

lands are the potential hotspots of GHG emission. Thus, it is important to study GHG emission to obtain a comprehensive picture of the role of the riparian wetlands in climate change.

We roughly estimated the annual cumulative emission amounts of CO_2 , CH_4 , and N_2O from the riparian wetlands and hillslope grasslands around the Xilin River basin and further calculated their global warming potential. As Table 6 indicates, annual cumulative emissions of CO_2 and CH_4 decreased in the following order: upstream riparian wetlands > downstream riparian wetlands > hillslope grasslands. N_2O decreased in the following order: upstream riparian wetlands > hillslope grasslands > downstream riparian wetlands. In this study, we used the static dark-box method to measure CO_2 emissions, which does not consider the absorption and fixation of CO_2 by plant photosynthesis. Therefore, the total annual cumulative CO_2 emissions are high. This result clearly showed the more significant impact of CO_2 emission than that of CH_4 and N_2O emissions on global warming. The GWP depends on the cumulative emissions of the GHGs. The GWPs, shown in Table 6, were in the following order: upstream riparian wetlands ($13\,474.91\text{ kg hm}^{-2}$) > downstream riparian wetlands ($8974.12\text{ kg hm}^{-2}$) > hillslope grasslands ($8351.24\text{ kg hm}^{-2}$). Therefore, both the riparian wetlands and the grasslands are the “sources” of GHGs on a 100-year timescale. The source strength of the wetlands is higher than that of the grasslands, further indicating that the riparian wetlands are hotspots of GHG emission.

4.3 Effects of riparian wetland degradation on GHG emissions

The hydrology and soil properties showed evident differences between transects because the downstream zone was dry all year due to the presence of the Xilinhot Dam (Fig. 1). The dam caused the degradation of the riparian wetlands, resulting in reduced GHG emission. The average CO_2 emission amounted to $1663\text{ mg m}^{-2}\text{ h}^{-1}$ in the upstream transects (T1, T2, and T3) at the riparian wetlands, while the downstream transects (T4 and T5) recorded an average emission of $1084\text{ mg m}^{-2}\text{ h}^{-1}$, 35% lower than that in the upstream transects. The N_2O emission from the riparian wetlands was lower in the downstream transects.

Wetland degradation first resulted in the continuous reduction of SMC, which led to the deepening of the wetland’s aerobic layer thickness. Besides, SMC may affect ST and thus transport the CH_4 emissions from a source to a sink by affecting methanogen activity (Yan et al., 2018). Second, the reduction of SMC impeded physiological activities of aboveground plants and inhabited related enzyme activities in the respiration process. Meanwhile, various enzyme reactions of underground microorganisms under water stress influence and reduced CO_2 emissions (Zhang et al., 2017). Finally, after wetland degradation, long-term drought led to an extremely low SMC, which is not conducive to the growth of nitrifying and denitrifying bacteria and causes the transport of N_2O emissions from source to sink (Zhu et al., 2013). As Table 1 shows, soil TOC content in the upstream transects (average: 25.1 g kg^{-1}) was higher than that in the down-

Table 5. GHG emission fluxes of riparian wetlands and grasslands.

Sample plot		GHG emissions in August ($\text{mg m}^{-2} \text{h}^{-1}$)			GHG emissions in October ($\text{mg m}^{-2} \text{h}^{-1}$)			Reference
		CO ₂	CH ₄	N ₂ O	CO ₂	CH ₄	N ₂ O	
Wetlands of upstream transects (T1, T2, and T3)	$n = 13$	1606.28 ± 697.78	1.417 ± 3.41	0.031 ± 0.03	182.35 ± 88.26	0.272 ± 0.49	0.002 ± 0.005	This study
Wetlands of downstream transects (T4 and T5)	$n = 7$	1144.15 ± 666.50	-0.215 ± 0.45	-0.037 ± 0.05	98.13 ± 15.11	-0.015 ± 0.05	0.001 ± 0.01	
Hillslope grasslands of all transects	$n = 7$	1071.54 ± 225.39	-0.300 ± 0.40	0.003 ± 0.03	77.68 ± 25.32	-0.048 ± 0.03	-0.002 ± 0.005	
Meadow grassland		166.39 ± 45.89	-0.038 ± 0.009	0.002 ± 0.001	–	–	–	Guo et al. (2017)
Typical grassland		240.32 ± 87.56	-0.042 ± 0.025	0.037 ± 0.034	–	–	–	
Desert grassland		107.59 ± 54.10	-0.036 ± 0.015	0.003 ± 0.001	–	–	–	
Typical grassland		520.25 ± 59.07	-0.102 ± 0.012	0.007 ± 0.001	88.34 ± 9.84	-0.099 ± 0.003	0.005 ± 0.001	Zhang (2019)
Typical grassland		232.42 ± 18.90	-0.090 ± 0.005	0.004 ± 0.001	–	–	–	Chao (2019)
Typical grassland		265.23 ± 31.43	-0.185 ± 0.018	0.005 ± 0.001	189.41 ± 28.96	-0.092 ± 0.012	0.004 ± 0.001	
Meadow grassland		553.85	-0.163	0.003	47.73	-0.019	0.011	Geng (2004)
Typical grassland		308.60	-0.105	0.002	70.25	-0.029	0.007	

Table 6. Cumulative annual emission flux and global warming potential of GHGs in riparian wetlands and grasslands.

Sample plot	CO ₂ /kg hm ⁻²	CH ₄ /kg hm ⁻²	N ₂ O/kg hm ⁻²	GWP/CO ₂ kg hm ²
Wetlands of upstream transects (T1, T2, and T3)	13092.80 ± 5378.16	12.36 ± 26.40	0.25 ± 0.23	13474.91 ± 5828.68
Wetlands of downstream transects (T4 and T5)	9093.47 ± 4831.82	-1.68 ± 3.23	-0.26 ± 0.40	8974.12 ± 4912.75
Hillslope grasslands of all transects	8412.26 ± 1614.26	-2.55 ± 3.12	0.01 ± 0.20	8351.24 ± 1648.22

stream transects (average: 8.41 g kg⁻¹). The relatively low SMC and the aerobic environment were conducive to the mineralization and decomposition of the TOC. The degradation of plants in the wetlands led to the gradual reduction of BIO. Ultimately, the plant carbon source input of the degraded wetlands decreased, and the bare land temperature increased due to the reduced plant shelter. This accelerated the decomposition of TOC, leading to its decrease. This result indicates that wetland degradation caused the soil carbon pool's loss and weakened the wetland carbon source–sink function. These results are in agreement with those of Xia et al. (2017).

The degraded wetlands also caused soil desertification and salinization, leading to a decline in the physical protection afforded by organic carbon and a reduction in soil aggregates. Thus, the preservative effect provided by organic carbon declined. The TOC content and SMC in the dry lake bed in transect T5 were relatively high; however, the GHG emission was very low along this transect because soil pH values increased after the degradation of the lake soil, exceeding the optimum range required for microorganism activity. The soil C : N ratio was very high, resulting in severe mineralization and a low microbial decomposition rate, thus affecting the GHG emissions.

5 Conclusions

The riparian wetlands in the Xilin River basin constitute a dynamic ecosystem. The present spatial and temporal transfers in the studied biogeochemical processes were attributed to the changes in SMC, ST, and soil substrate availability. Our simultaneous analysis of CO₂, CH₄, and N₂O emissions from the riparian wetlands and the hillslope grasslands in the Xilin River basin revealed that the majority of the GHG emissions occurred in the form of CO₂. Moreover, our results clearly illustrate a marked seasonality and spatial pattern of GHG emissions along the transects and in the longitudinal direction (i.e., upstream and downstream). SMC and ST were two critical factors controlling the GHG emissions. Moreover, the abundant BIO promoted the CO₂, CH₄, and N₂O emissions.

The riparian wetlands are potential hotspots of GHG emissions in the Inner Mongolian region. However, the degradation of these wetlands has transformed the area from a source to a sink for CH₄ and N₂O emissions and reduced CO₂ emissions, which has severely affected the wetland carbon cycle processes. Our results show that though the riparian wetlands have high CO₂ emissions, the wetlands are CO₂ sinks due to the photosynthesis of plants. Overall, our study suggests that anthropogenic activities have significantly changed the hydrological characteristics of the studied area and that this can accelerate carbon loss from the riparian wetlands and further influence GHG emissions in the future.

Data availability. All relevant data are included as graphics and tables in the paper. All raw data will be made available on request.

Author contributions. XinL, XixL, and RY designed the research framework and wrote the manuscript. XXL and RHY supervised the study. XinL, HX, ZQ, ZC, and ZZ carried out the field experiments and laboratory analyses. ZZ drew the GIS mapping in this paper. TL proofread a previous version of the manuscript. HS contributed much to the revised version of our manuscript.

Competing interests. The authors declare that they have no conflict of interest.

Disclaimer. Publisher's note: Copernicus Publications remains neutral with regard to jurisdictional claims in published maps and institutional affiliations.

Acknowledgements. This study was funded by the National Key Research and Development Program of China (grant no. 2016YFC0500508), Major Science and Technology Projects of Inner Mongolia Autonomous Region (grant nos. 2020ZD0009 and ZDZX2018054), National Natural Science Foundation of China

(grant no. 51869014), Key Scientific and Technological Project of Inner Mongolia (grant no. 2019GG019), and Open Project Program of the Ministry of Education Key Laboratory of Ecology and Resources Use of the Mongolian Plateau (grant no. KF2020006). We thank Wiley Editing Services (<http://wileyeditingservices.com>, last access: 24 June 2021) for its linguistic assistance during the preparation of a previous version of this paper.

Financial support. This research has been supported by the National Key Research and Development Program of China (grant no. 2016YFC0500508), the National Natural Science Foundation of China (grant no. 51869014), the Science and Technology Major Project on Lakes of Inner Mongolia (grant nos. 2020ZD0009 and ZDZX2018054), Key Scientific and Technological Project of Inner Mongolia (grant no. 2019GG019), and Open Project Program of the Ministry of Education Key Laboratory of Ecology and Resources Use of the Mongolian Plateau (grant no. KF2020006).

Review statement. This paper was edited by Anja Rammig and reviewed by two anonymous referees.

References

- Azam, F., Gill, S., and Farooq, S.: Availability of CO₂ as a factor affecting the rate of nitrification in soil, *Soil Biol. Biochem.*, 37, 2141–2144, <https://doi.org/10.1016/j.soilbio.2005.02.036>, 2005.
- Baggs, E. M., Richter, M., Cadisch, G., and Hartwig, U. A.: Denitrification in grass swards is increased under elevated atmospheric CO₂, *Soil Biol. Biochem.*, 35, 729–732, [https://doi.org/10.1016/S0038-0717\(03\)00083-X](https://doi.org/10.1016/S0038-0717(03)00083-X), 2003.
- Beger, M., Grantham, H. S., Pressey, R. L., Wilson, K. A., Peterson, E. L., Dorfman, D., Lourival, R., Brumbaugh, D. R., and Possingham, H. P.: Conservation planning for connectivity across marine, freshwater, and terrestrial realms, *Biol. Conserv.*, 143, 565–575, <https://doi.org/10.1016/j.biocon.2009.11.006>, 2010.
- Brady, N. C.: Nature and properties of soils, Prentice-Hall, Inc., Wichita, USA, <https://doi.org/10.2307/3894608>, 1999.
- Cao, M., Yu, G., Liu, J., and Li, K.: Multi-scale observation and cross-scale mechanistic modelling on terrestrial ecosystem carbon cycle, *Sci. China Ser. D*, 48, 17–32, 2005.
- Chao, R.: Effects of Simulated Climate Change on Greenhouse Gas Fluxes in Typical Steppe Ecosystem, MS thesis, Inner Mongolia University, Hohhot, China, 2019.
- Cheng, S. and Huang, J.: Enhanced soil moisture drying in transitional regions under a warming climate, *J. Geophys. Res.-Atmos.*, 121, 2542–2555, <https://doi.org/10.1002/2015JD024559>, 2016.
- Christensen, S., Simkins, S., and Tiedje, J. M.: Temporal Patterns of Soil Denitrification: Their Stability and Causes, *Soil Sci. Soc. Am. J.*, 54, 1614, <https://doi.org/10.2136/sssaj1990.03615995005400060017x>, 1990.
- Ding, W., Cai, Z., and Tsuruta, H.: Cultivation, nitrogen fertilization, and set-aside effects on methane uptake in a drained marsh soil in Northeast China, *Glob. Change Biol.*, 10, 1801–1809, <https://doi.org/10.1111/j.1365-2486.2004.00843.x>, 2010.

- Enwall, K., Philippot, L., and Hallin, S.: Activity and composition of the denitrifying bacterial community respond differently to long-term fertilization, *Appl. Environ. Microb.*, 71, 8335–8343, <https://doi.org/10.1128/AEM.71.12.8335-8343.2005>, 2005.
- Fan, X.: Research on nitrification potential and denitrification potential of soil in several farmland in China, Nanjing Institute of Soil Sciences, PhD thesis, Chinese Academy of Sciences, Nanjing, China, 1995.
- Ferrón, S., Ortega, T., Gómez-Parra, A., and Forja, J. M.: Seasonal study of dissolved CH₄, CO₂ and N₂O in a shallow tidal system of the bay of Cádiz (SW Spain), *J. Marine Syst.*, 66, 244–257, <https://doi.org/10.1016/j.jmarsys.2006.03.021>, 2007.
- Geng, H.: Study on Characters of CO₂, CH₄, N₂O Fluxes and the Relationship between Them and Environmental Factors in the Temperate Typical Grassland Ecosystem, MS thesis, Northwest Agriculture & Forestry University, Yangling, China, 2004.
- Gholz, H. L., Wedin, D. A., Smitherman, S. M., Harmon, M. E., and Parton, W. J.: Long-term dynamics of pine and hardwood litter in contrasting environments: toward a global model of decomposition, *Glob. Change Biol.*, 6, 751–765, <https://doi.org/10.1046/j.1365-2486.2000.00349.x>, 2000.
- Gou, Q., Qu, J., Wang, G., Xiao, J., and Pang, Y.: Progress of wetland researches in arid and semi-arid regions in China, *Arid Zone Research*, 32, 213–220, 2015.
- Guo, X., Zhou, D., and Li, Y.: Net Greenhouse Gas Emission and Its Influencing Factors in Inner Mongolia Grassland, Chinese Grassland Society, Guangzhou, China, 2017.
- Heilman, J. L., Cobos, D. R., Heinsch, F. A., Campbell, C. S., and McInnes, K. J.: Tower-based conditional sampling for measuring ecosystem-scale carbon dioxide exchange in coastal wetlands, *Estuaries*, 22, 584–591, <https://doi.org/10.2307/1353046>, 1999.
- Hui, R. N.: Study on the emission of CO₂ and its impact factors in riparian wetland, MS thesis, Northeast Forestry University, 23 pp., 2014.
- Inubushi, K., Furukawa, Y., Hadi, A., Purnomo, E., and Tsuruta, H.: Seasonal changes of CO₂, CH₄ and N₂O fluxes in relation to land-use change in tropical peatlands located in coastal area of South Kalimantan, *Chemosphere*, 52, 603–608, [https://doi.org/10.1016/s0045-6535\(03\)00242-x](https://doi.org/10.1016/s0045-6535(03)00242-x), 2003.
- IPCC: Climate Change 2013: The Physical Science Basis. Contribution of Working Group I of the IPCC, 43, 866–871, 2013.
- Jacinte, P. A., Vidon, P., Fisher, K., Liu, X., and Baker, M. E.: Soil Methane and Carbon Dioxide Fluxes from Cropland and Riparian Buffers in Different Hydrogeomorphic Settings, *J. Environ. Qual.*, 44, 1080–1115, <https://doi.org/10.2134/jeq2015.01.0014>, 2015.
- Johnson-Randall, L. A. and Foote, A. L.: Effects of managed impoundments and herbivory on wetland plant production and stand structure, *Wetlands*, 25, 38–50, [https://doi.org/10.1672/0277-5212\(2005\)025\[0038:EOMIAH\]2.0.CO;2](https://doi.org/10.1672/0277-5212(2005)025[0038:EOMIAH]2.0.CO;2), 2005.
- Koops, J. G., Oenema, O., and Beusichem, M. L.: Denitrification in the top and sub soil of grassland on peat soils, *Plant Soil*, 184, 1–10, <https://doi.org/10.1007/bf00029269>, 1996.
- Kou, X.: Study on Soil Physicochemical Properties and Bacterial Community Characteristics of River Riparian Wetland in Inner Mongolia Grassland, MS thesis, Inner Mongolia University, Hohhot, China, 2018.
- Liu, C.: Effects of Nitrogen Addition on the CO₂ Emissions in the Reed (*Phragmites australis*) Wetland of the Yellow River Delta, China, MS thesis, Liaocheng University, Liaocheng, China, 2019.
- Liu, C., Xie, G., and Huang, H.: Shrinking and drying up of Baiyangdian Lake wetland: a natural or human cause?, *Chinese Geogr. Sci.*, 16, 314–319, 2006.
- Liu, F., Liu, C., Wang, S., and Zhu, Z.: Correlations among CO₂, CH₄, and N₂O concentrations in soil profiles in central Guizhou Karst area, *Chinese Journal of Ecology*, 29, 717–723, [https://doi.org/10.1016/S1872-5813\(11\)60001-7](https://doi.org/10.1016/S1872-5813(11)60001-7), 2010.
- Liu, J., Wang, J., Li, Z., Yu, J., Zhang, X., Wang, C., and Wang, Y.: N₂O Concentration and Its Emission Characteristics in Sanjiang Plain Wetland, *Chinese Journal of Environmental Science*, 24, 33–39, 2003.
- Lu, Y., Song, C., Wang, Y., and Zhao, Z.: Influence of plants on CO₂ and CH₄ emission in wetland ecosystem, *Acta Botanica Boreali-Occidentalia Sinica*, 27, 2306–2313, 2007.
- Lu, Z., Du, R., Du, P., Li, Z., Liang, Z., Wang, Y., Qin, S., and Zhong, L.: Effect of mowing on N₂O and CH₄ fluxes emissions from the meadow-steppe grasslands of Inner Mongolia, *Front. Earth Sci.*, 9, 473–486, <https://doi.org/10.1007/s11707-014-0486-z>, 2015.
- Lv, M., Sheng, L., and Zhang, L.: A review on carbon fluxes for typical wetlands in different climates of China, *Wetland Science*, 11, 114–120, <https://doi.org/10.13248/j.cnki.wetlandsci.2013.01.001>, 2013.
- Mahl, S. S. and McGill, W. B.: Nitrification in three Alberta soils: effects of temperature, moisture and substrates concentration, *Soil Biol. Biochem.*, 14, 393–399, [https://doi.org/10.1016/0038-0717\(82\)90011-6](https://doi.org/10.1016/0038-0717(82)90011-6), 1982.
- McLain, J. E. T. and Martens, D. A.: Moisture controls on trace gas fluxes in semiarid riparian soils, *Soil Sci. Soc. Am. J.*, 70, 367, <https://doi.org/10.2136/sssaj2005.0105>, 2006.
- Meng, W., Wu, D., and Wang, Z.: Control factors and critical conditions between carbon sinking and sourcing of wetland ecosystem, *Ecology and Environmental Sciences*, 20, 1359–1366, [https://doi.org/10.1016/S1671-2927\(11\)60313-1](https://doi.org/10.1016/S1671-2927(11)60313-1), 2011.
- Mitsch, W. J. and Gosselink, J. G.: *Wetlands* (Fourth Edition), John Wiley & Sons Inc., Hoboken, NJ, 2007.
- Mitsch, W. J., Gosselink, J. G., Zhang, L., and Anderson, C. J.: *Wetland ecosystems*, John Wiley & Sons, New Jersey, USA, 2009.
- Moldrup, P., Olesen, T., Schjønning, P., Yamaguchi, T., and Rolston, D. E.: Predicting the gas diffusion coefficient in undisturbed soil from soil water characteristics, *Soil Sci. Soc. Am. J.*, 64, 1588–1594, <https://doi.org/10.2136/sssaj2000.64194x>, 2000.
- Morley, N. and Baggs, E. M.: Carbon and oxygen controls on N₂O and N₂ production during nitrate reduction, *Soil Biol. Biochem.*, 42, 1864–1871, <https://doi.org/10.1016/j.soilbio.2010.07.008>, 2010.
- Naiman, R. J. and Decamps, H.: The ecology of interfaces: Riparian zones, *Annu. Rev. Ecol. Syst.*, 28, 621–658, <https://doi.org/10.1146/annurev.ecolsys.28.1.621>, 1997.
- National Agricultural Technology Extension Service Center (NATESC): Technical specification for soil analysis, China Agriculture Press, Beijing, China, 256 pp., ISBN 978-71-0910-925-9, 2006.
- Niu, C., Wang, S., Guo, Y., Liu, W., and Zhang, J.: Studies on variation characteristics of soil nitrogen forms, nitrous oxide emis-

- sion and nitrogen storage of the *Phragmites australis*-dominated land/inland water ecotones in Baiyangdian wetland, *Journal of Agricultural University of Hebei*, 40, 72–79, 2017.
- Pierzynski, G. M., Vance, G. F., and Sims, T. J.: *Soils and Environmental Quality*, 3rd Edn., CRC Press Inc., Boca Raton, 592 pp., <https://doi.org/10.1201/b12786>, 2005.
- Poblador, S., Lupon, A., Sabaté, S., and Sabater, F.: Soil water content drives spatiotemporal patterns of CO₂ and N₂O emissions from a Mediterranean riparian forest soil, *Biogeosciences*, 14, 4195–4208, <https://doi.org/10.5194/bg-14-4195-2017>, 2017.
- Qin, S., Tang, J., Pu, J., Xu, Y., Dong, P., Jiao, L., and Guo, J.: Fluxes and influencing factors of CO₂ and CH₄ in Hangzhou Xixi Wetland, China, *Earth and Environment*, 44, 513–519, 2016.
- Rückauf, U., Augustin, J., Russow, R., and Merbach, W.: Nitrate removal from drained and reflooded fen soils affected by soil N transformation processes and plant uptake, *Soil Biol. Biochem.*, 36, 77–90, <https://doi.org/10.1016/j.soilbio.2003.08.021>, 2004.
- Sjögersten, S., Wal, R. V. D., and Woodin, S. J.: Small-scale hydrological variation determines landscape CO₂ fluxes in the high Arctic, *Biogeochemistry*, 80, 205–216, <https://doi.org/10.1007/s10533-006-9018-6>, 2006.
- Sun, Y., Wu, H., and Wang, Y.: The influence factors on N₂O emissions from nitrification and denitrification reaction, *Ecology and Environmental Sciences*, 20, 384–388, <https://doi.org/10.1631/jzus.B1000275>, 2011.
- Tong, C., Wu, J., Yong, S., Yang, J., and Yong, W.: A landscape-scale assessment of steppe degradation in the Xilin River Basin, Inner Mongolia, China, *J. Arid Environ.*, 59, 133–149, <https://doi.org/10.1016/j.jaridenv.2004.01.004>, 2004.
- Waddington, J. M. and Roulet, N. T.: Carbon balance of a boreal patterned peatland, *Glob. Change Biol.*, 6, 87–97, <https://doi.org/10.1046/j.1365-2486.2000.00283.x>, 2000.
- Whiting, G. J. and Chanton, J. P.: Greenhouse carbon balance of wetlands: methane emission versus carbon sequestration, *Tellus B*, 53, 521–528, <https://doi.org/10.3402/tellusb.v53i5.16628>, 2001.
- WMO: WMO Statement on the State of the Global Climate in 2017, World Meteorological Organization, 2018.
- Xi, X., Zhu, Z., and Hao, X.: Spatial variability of soil organic carbon in Xilin River Basin, *Research of Soil and Water Conservation*, 24, 97–104, 2017.
- Xia, P., Yu, L., Kou, Y., Deng, H., and Liu, J.: Distribution characteristics of soil organic carbon and its relationship with enzyme activity in the Caohai wetland of the Guizhou Plateau, *Acta Scientiae Circumstantial*, 37, 1479–1485, <https://doi.org/10.13671/j.hjkxxb.2016.0129>, 2017.
- Xu, H., Cai, Z., and Yagi, K.: Methane Production Potentials of Rice Paddy Soils and Its Affecting Factors, *Acta Pedologica Sinica*, 45, 98–104, <https://doi.org/10.1163/156939308783122788>, 2008.
- Yan, L., Zhang, X., Wang, J., Li, Y., Wu, H., and Kang, X.: Drainage effects on carbon flux and carbon storage in swamps, marshes, and peatlands, *Chin. J. Appl. Environ. Biol.*, 24, 1023–1031, <https://doi.org/10.19675/j.cnki.1006-687x.2017.11031>, 2018.
- Yu, P., Zhang, J., and Lin, C.: Progress of influence factors on N₂O emission in farmland soil, *Environment and Sustainable Development*, 5, 20–22, 2006.
- Zhang, D.: Effects of Different Grazing Intensities on Greenhouse Gases Flux in Typical Steppe of Inner Mongolia, MS thesis, Inner Mongolia University, Hohhot, China, 2019.
- Zhang, Y., Hao, Y., Cui, L., Li, W., Zhang, X., Zhang, M., Li, L., Yang, S., and Kang, X.: Effects of extreme drought on CO₂ fluxes of Zoige alpine peatland, *Journal of University of Chinese Academy of Sciences*, 34, 462–470, 2017.
- Zhang, Z., Hua, L., Yin, X., Hua, L., and Gao, J.: Nitrous oxide emission from agricultural soil land some influence factors, *Journal of Capital Normal University: Natural Science Edition*, 26, 114–120, 2005.
- Zhu, X., Song, C., Guo, Y., Shi, F., and Wang, L.: N₂O emissions and its controlling factors from the peatlands in the Sanjiang Plain, *China Environmental Sciences*, 33, 2228–2234, 2013.
- Zona, D., Oechel, W. C., Kochendorfer, J., Paw, U. K. T., Salyuk, A. N., Olivas, P. C., Oberbauer, S. F., and Lipson, D. A.: Methane fluxes during the initiation of a large-scale water table manipulation experiment in the Alaskan Arctic tundra, *Global Biogeochem. Cy.*, 23, GB2013, <https://doi.org/10.1029/2009gb003487>, 2009.